

Two-step growth of VSe_2 films and their photoelectric properties

Yu Zeng(曾玉), Shengli Zhang(张生利), Xiuling Li(李秀玲), Jianping Ao(敖建平), Yun Sun(孙云), Wei Liu(刘玮), Fangfang Liu(刘芳芳), Peng Gao(高鹏), Yi Zhang(张毅)

Citation: Chin. Phys. B . 2019, 28(5): 058101. **doi:** 10.1088/1674-1056/28/5/058101
Journal homepage: http://cpb.iphy.ac.cn; http://iopscience.iop.org/cpb

What follows is a list of articles you may be interested in

Structural and electrical properties of reactive magnetron sputtered yttrium-doped HfO_2 films

Yu Zhang(张昱), Jun Xu(徐军), Da-Yu Zhou(周大雨), Hang-Hang Wang(王行行), Wen-Qi Lu(陆文琪), Chi-Kyu Choi
Chin. Phys. B . 2018, 27(4): 048103. **doi:** 10.1088/1674-1056/27/4/048103

Positive gate bias stress-induced hump-effect in elevated-metal metal-oxide thin film transistors

Dong-Yu Qi(齐栋宇), Dong-Li Zhang(张冬利), Ming-Xiang Wang(王明湘)
Chin. Phys. B . 2017, 26(12): 128101. **doi:** 10.1088/1674-1056/26/12/128101

Influence of Ag and Sn incorporation in In_2S_3 thin films

Lin Ling-Yan, Yu Jin-Ling, Cheng Shu-Ying, Lu Pei-Min
Chin. Phys. B . 2015, 24(7): 078103. **doi:** 10.1088/1674-1056/24/7/078103

High-crystalline GaSb epitaxial films grown on GaAs(001) substrates by low-pressure metal-organic chemical vapor deposition

Wang Lian-Kai, Liu Ren-Jun, Lü You, Yang Hao-Yu, Li Guo-Xing, Zhang Yuan-Tao, Zhang Bao-Lin
Chin. Phys. B . 2015, 24(1): 018102. **doi:** 10.1088/1674-1056/24/1/018102

Characterization of zirconium thin films deposited by pulsed laser deposition

Liu Wei, Wan Jing-Ping, Cai Wu-Peng, Liang Jian-Hua, Zhou Xiao-Song, Long Xing-Gui
Chin. Phys. B . 2014, 23(9): 098103. **doi:** 10.1088/1674-1056/23/9/098103

Two-step growth of VSe_2 films and their photoelectric properties*

Yu Zeng(曾玉)[1], Shengli Zhang(张生利)[1], Xiuling Li(李秀玲)[1], Jianping Ao(敖建平)[1], Yun Sun(孙云)[1], Wei Liu(刘玮)[1], Fangfang Liu(刘芳芳)[1], Peng Gao(高鹏)[2], and Yi Zhang(张毅)[1,†]

[1] *Institute of Photoelectronic Thin Film Devices and Technology, Tianjin Key Laboratory of Photoelectronic Thin Film Devices and Technology, Tianjin* 300071, *China*
[2] *Tianjin Institute of Power Source, Tianjin* 300384, *China*

(Received 1 February 2019; revised manuscript received 28 February 2019; published online 4 April 2019)

We put forward a two-step route to synthesize vanadium diselenide (VSe_2), a typical transition metal dichalcogenide (TMD). To obtain the VSe_2 film, we first prepare a vanadium film by electron beam evaporation and we then perform selenization in a vacuum chamber. This method has the advantages of low temperature, is less time-consuming, has a large area, and has a stable performance. At 400 °C selenization temperature, we successfully prepare VSe_2 films on both glass and Mo substrates. The prepared VSe_2 has the characteristic of preferential growth along the *c*-axis, with low transmittance. It is found that the contact between Al and VSe_2/Mo is ohmic contact. Compared to Mo substrate, lower square resistance and higher carrier concentration of the VSe_2/Mo sample reveal that the VSe_2 film may be a potential material for thin film solar cells or other semiconductor devices. The new synthetic strategy that is developed here paves a sustainable way to the application of VSe_2 in photovoltaic devices.

Keywords: two-step route, VSe_2, selenization, thin film

PACS: 81.10.Pq, 81.15.–z, 81.15.Dj, 81.20.–n **DOI:** 10.1088/1674-1056/28/5/058101

1. Introduction

Transition metal dichalcogenides (TMDs) materials, which exhibit unique structural features and intriguing properties, have attracted much attention recently.[1–4] As a typical transition metal dichalcogenide, vanadium diselenide (VSe_2) is made up of Se–V–Se layers.[5,6] Compared to the semiconducting $MoSe_2$ and other TMDs, VSe_2 is metallic in nature due to the strong electron coupling interaction for all neighboring V^{4+}–V^{4+} pairs.[7] In addition, VSe_2 shows intrinsic ferromagnetism behavior[8,9] and extra-high electrical conductivity.[10]

However, most of the VSe_2 reports are related to their electromagnetic properties, and its application in optoelectronic devices is rare. The main challenge limiting the application of VSe_2 in this respect is the limitation of its preparation method. Over the past few decades, many methods to prepare VSe_2 have been suggested. The VSe_2 was first prepared in the tube furnace at high temperature.[11,12] At present, the synthesis method of chemical vapor transport (CVT) usually requires a long reaction time (72–120 h) and a high reaction temperature (800-900 °C).[13–15] Compared with other methods, the chemical vapor deposition (CVD) method should be the best choice for preparing the high crystalline quality VSe_2.[10,16–20] However, it also needs high reaction temperature and long reaction time. To prepare VSe_2 at low temperature, aqueous solution was used to synthesize the bulk VSe_2 for the first time by Xu *et al.*[6] Other groups have proposed different chemical-based methods to synthesize VSe_2, such as one-pot solvothermal method,[21] hydrothermal method,[7,22,23] and one-pot colloidal method.[5] However, these wet methods of preparing VSe_2 have not been widely used because of the complex chemical environment in solution.

Herein, we put forward a two-step method to prepare VSe_2 films. This method has the advantages of low temperature, large area, and stable performance. Simultaneously, the reaction time is very short. In our synthesis, non-toxic vanadium metal column and Se powder are used as the metal sources. In the first step, we use electron beam evaporation to obtain a vanadium film. In the second step, the vanadium film is selenized in a closed vacuum chamber. We not only successfully prepare VSe_2 films on the glass substrates, but also obtain dense VSe_2 films on the Mo substrates. This two-step process for preparing VSe_2 proposed in this paper can be compatible with the fabrication process of many optoelectronic devices; for example, VSe_2 can be used as a back contact layer between CdTe or CZTSSe and back electrodes.[24,25]

2. Experimental details

The two-step synthesizing procedure of VSe_2 flakes is schematically depicted in Fig. 1(a). First, we prepared a V film by electron beam evaporation on a glass substrate. Main-

*Project supported by the National Natural Science Foundation of China (Grant Nos. 51572132, 61674082, and 61774089), the National Key R&D Program of China (Grant No. 2018YFB1500202), Tianjin Natural Science Foundation of Key Project, China (Grant Nos. 18JCZDJC31200 and 16JCZDJC30700), Yang Fan Innovative and Entrepreneurial Research Team Project, China (Grant No. 2014YT02N037), 111 Project, China (Grant No. B16027), and the International Cooperation Base, China (Grant No. 2016D01025).

†Corresponding author. E-mail: yizhang@nankai.edu.cn

© 2019 Chinese Physical Society and IOP Publishing Ltd

taining the same vacuum pressure of 1×10^{-3} Pa, 50 nm thick V film was prepared on glass after 10 min pre-evaporation (to evaporate the surface oxides). Then, the V film was selenized in a closed vacuum chamber, as shown in Fig. 1(b). The sample to be selenized was put into the box filled with selenium powder. The vacuum pressure of the vacuum chamber was 1.0×10^{-3} Pa, and a certain amount of Ar gas was introduced for the purpose of preventing the metal V film from being oxidized during the high temperature selenization process. We provided sufficient selenium (2 g of selenium powder) to prevent selenium deficiency. It has been reported that it is helpful to prevent the vanadium film from being oxidized under the excessive selenium atmosphere.[26]

The specific selenization process is shown in Fig. 2(a). The substrate and the selenium source were simultaneously raised from room temperature to the same selenization temperature of 550 °C, which took 10 min. After 30 min of constant temperature, the selenium source started to cool down naturally. To prevent the substrate temperature from falling too fast and the condensed Se being absorbed onto the surface of the sample, we let the substrate be kept at a constant temperature for 15 min more than the selenium source and we also performed a degassing process when the substrate temperature was lowered from 550 °C to 300 °C.

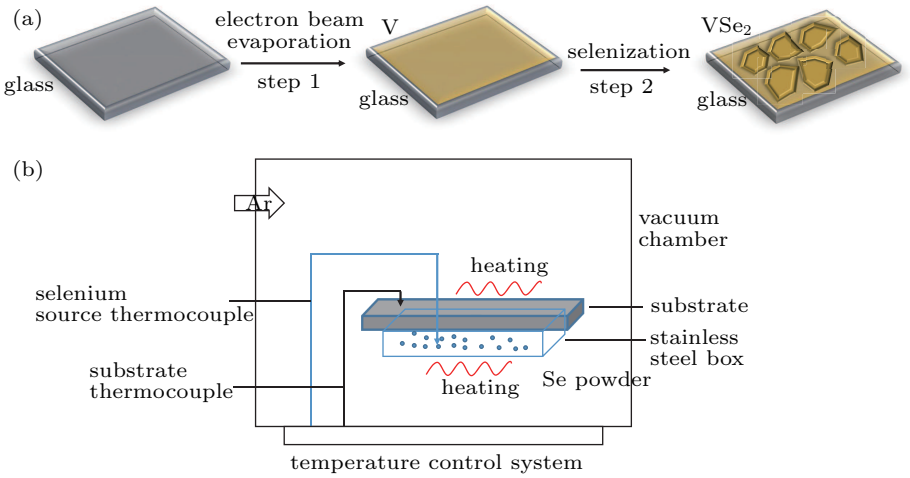


Fig. 1. (a) Schematic diagram of the synthesization of the VSe_2 film with two-step method, (b) schematic diagram of the vacuum chamber for selenization process.

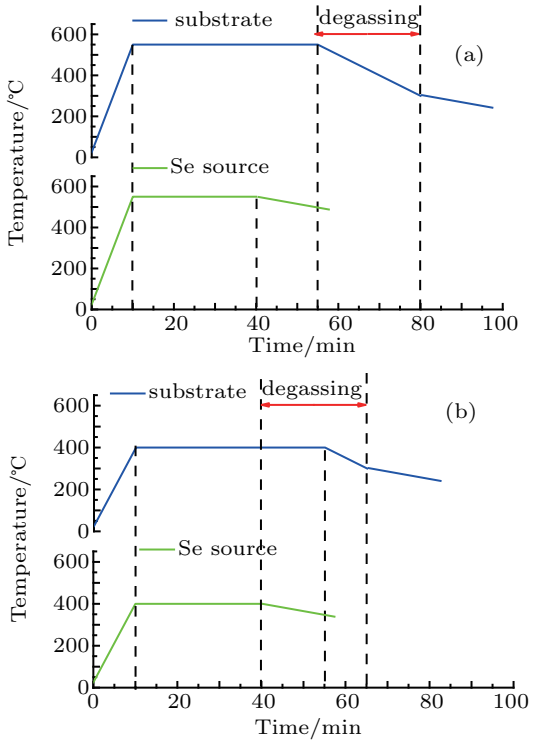


Fig. 2. (a) Selenization process at a selenization temperature of 550 °C and (b) at a temperature of 400 °C.

The phase structures of the films were measured by the PANalytical X'Pert pro x-ray diffractometer (XRD), which used Cu-$K\alpha$ (0.15418 nm) as the radiation source. The surface and profile of the films were observed by a Hitachi S-4800 field emission scanning electron microscope (SEM). The thickness of the films was measured by Ambios XP-2 model profiler. The current–voltage (J–V) curve was measured by a solar simulator under the standard AM1.5 spectrum with illumination intensity of 1000 W·m^{-2} at room temperature. The optical properties of the films were observed by Varian's Cary 5000 model UV–Vis–NIR spectrophotometer. The electrical properties of the films were measured by the Accent Optics Technology HL5550 Model Hall effect test system. X-ray photoelectron spectroscopy (XPS, Thermo Fisher ESCALAB 250 Xi) was used to detect the sample components. The excitation source used a monochromatic Al target (1486.6 eV) with an x-ray spot size of 500 μm.

3. Result and discussion

3.1. Preparation of VSe_2 thin film

Figure 3 shows the XRD pattern of the sample with 50 nm thick V film prepared on glass substrate at a selenization temperature of 550 °C. We can easily find the Se diffraction peak,

which indicates that Se vapor is easily condensed. Thus, the surface of the sample is rich in selenium. However, no VSe_2 peak is observed. A diffraction peak positioned at $2\theta = 33.0°$ belonging to V_3Se_4 is observed. It is obvious that the crystallinity of V_3Se_4 is not very good. Unfortunately, we also obtain VO_2. The appearance of oxide maybe because the oxygen in the air adhered to the surface of the V film before it was brought into the selenization chamber.

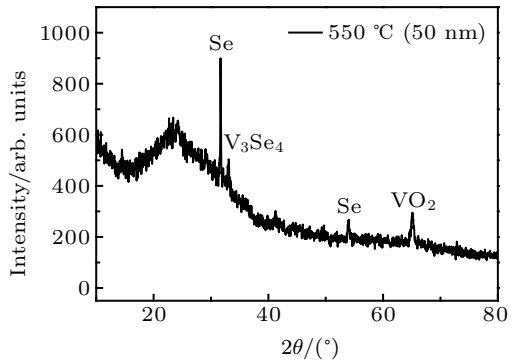


Fig. 3. XRD pattern of the sample with 50 nm thick V film selenized at 550 °C.

This experiment indicates that the selenization temperature is high. Then the selenization temperature was decreased to 400 °C. To prevent the appearance of Se on the surface of the film, the chamber is degassed as soon as the Se cools down, as shown in Fig. 2(b). Figure 4(a) shows the XRD pattern of a sample with 50 nm thick V film selenized at 400 °C. All the diffraction peaks can be indexed to the hexagonal VSe_2 phase (JCPDS card #01-089-1641) without any other phases. This result is consistent with other reports.[10,19,21] In order to verify the stability of the selenization process, we selenized a 100 nm thick V film deposited on the glass with the same selenization process. Figure 4(b) shows the XRD pattern. The crystal structure of the formed VSe_2 is confirmed to be a hexagonal phase without any impurity. The synthesized VSe_2 film highly (00*l*) prefers this orientation. In particular, the intensity of each diffraction peak is much stronger than that of the VSe_2 film prepared by selenizing the 50 nm V film. That is, the crystallinity of VSe_2 is well improved, and the VSe_2 preferential growth is along the *c*-axis. Figures 4(c) and 4(d) show the corresponding topographic images. Obviously, the sample obtained by selenizing a 50 nm thick V film is covered by some small nanosheets (Fig. 4(c)). The surface of the sample obtained by selenization of a 100 nm thick V film is covered with hexagonal nanosheets (Fig. 4(d)). These nanosheets on the surface of the sample grow very dense and have no holes or voids.

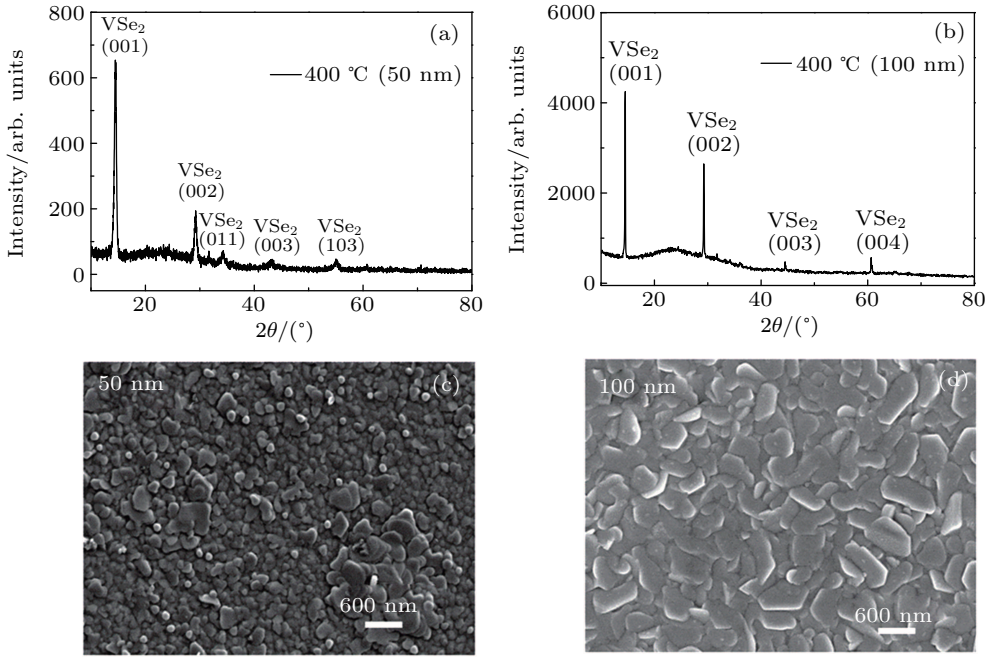


Fig. 4. XRD patterns and SEM images of the samples with (a), (c) 50 nm and (b), (d) 100 nm thick vanadium film selenized at 400 °C.

According to these results, VSe_2 can be prepared by selenizing 50 nm-thick V film at 400 °C. Then 50 nm thick V films were selenized at different temperatures to study the VSe_2 film growth behavior. Figure 5 shows the XRD patterns and the topographic SEM images of the corresponding films. At 350 °C, the XRD pattern exhibits a main diffraction peak (001) of VSe_2, which grows along with the *c*-axis direction. At such growth temperature, the film is composed of some light white particles and layered sheets. As the temperature increases to 400 °C, the film is still (001) preferred orientation. However, the intensity of the Bragg peak (001) is significantly enhanced (as shown in Fig. 5(b)), which means that

the crystal quality of VSe_2 is improved. The inset SEM image indicates that the film consists of large and well-crystallized nanosheets, which is consistent with the corresponding XRD result. As the temperature increases further, the intensity of the (001) peak decreases and the peaks of V_2O_3 are detected, as shown in Figs. 5(c) and 5(d). Specially, VSe_2 peaks cannot be detected and the film is composed of V_2O_3 entirely as the temperature increases to 500 °C. At such temperature, the films will not be composed of nanosheets, but small grains, as shown in the insets of Figs. 5(c) and 5(d). The oxidation of V should be the reason for the easier reaction between V and O_2 at such high temperature than that between V and Se vapor, where O_2 is possibility involved during transferring the formed V film from the growth chamber to the selenization chamber in atmosphere. These results indicate that the appropriate temperature for preparing the VSe_2 layer on the glass should be about 400 °C.

X-ray photoelectron spectroscopy (XPS) is carried out to further investigate the composition of the sample. The binding energies of 517.0 eV and 524.0 eV correspond to V $2p_{1/2}$ and $2p_{3/2}$, which indicate the V^{4+} state, as show in Fig. 6(a). The result is consistent with that in the references.[5,17,27] Figure 6(b) shows the XPS spectra of the Se 3d peak, the Se $3d_{5/2}$ (at 54.8 eV) and Se $3d_{3/2}$ (at 55.6 eV) peaks can be assigned to Se^{2-},[10,17,27,28] In addition, the binding energies (59.1 eV and 58.3 eV) of Se 3d match to those in SeO_2.[28] The appearance of SeO_2 can be considered as having some dangling bonds on the surface of the sample, and Se is combined with oxygen in the air to form a SeO_2 phase. The depth of the sample detected by the XPS test is only a few nanometers, so the SeO_2 phase can be clearly detected. We can conclude that the main component of the sample selenized at 400 °C is indeed VSe_2.

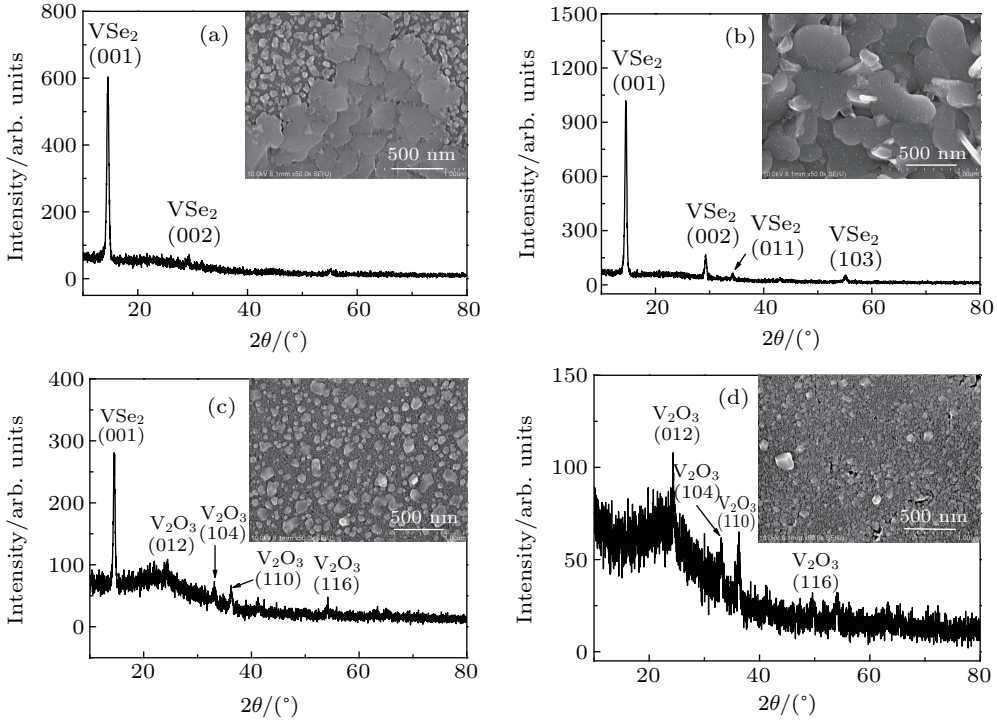


Fig. 5. XRD patterns of the V films selenized at (a) 350 °C, (b) 400 °C, (c) 450 °C, and (d) 500 °C, the inset shows the corresponding SEM images of the films.

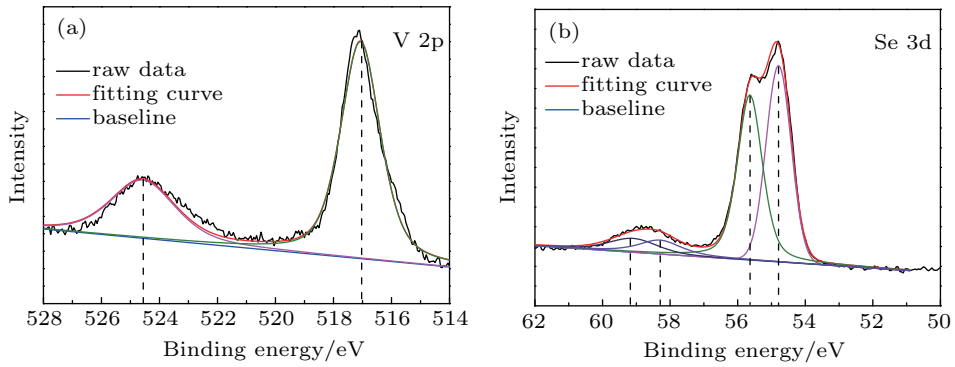


Fig. 6. XPS spectra of (a) V 2p and (b) Se 3d regions for the sample of the 50 nm thickness V films selenized at 400 °C.

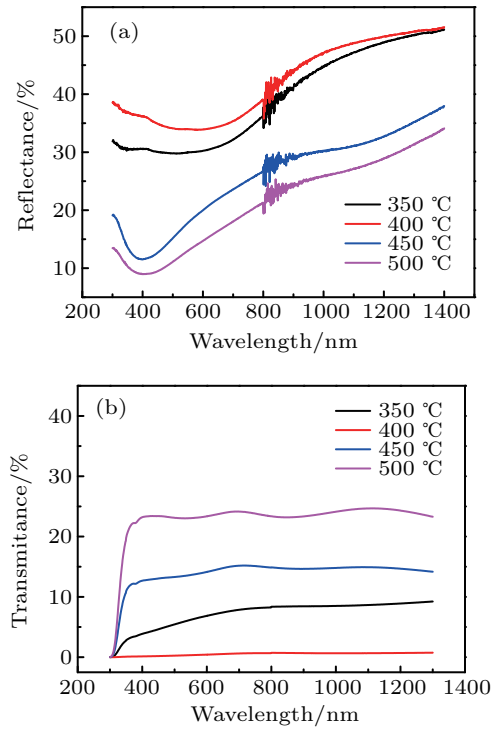


Fig. 7. (a) Reflection and (b) transmission spectra of V thin films annealed at different temperatures.

Optical properties of the as-grown thin films selenized at different temperatures are shown in Fig. 7. The sample of V thin film selenized at 400 °C has the highest reflectivity and the lowest transmittance. This indicates that VSe_2 formed by the two-step process can be used in optoelectronic devices, especially in photovoltaic devices. VSe_2 has the higher reflectivity and low transmittance. Because a VSe_2 thin film is deposited between the back contact and the absorber layer, it can promote the re-absorption of sunlight and reduce the loss of light, which will promote the collection of photo-generated carriers.

3.2. Electrical properties of VSe_2

If VSe_2 is used in a solar cell, such as the kesterite structured solar cell, then it will be grown on Mo back contact film. Considering that the excessive thickness of the VSe_2 layer deteriorates the performance of the device, we chose a 50 nm thick V film for research instead of 100 nm. Thus, we prepared a 50 nm thick V film on a Mo substrate. Both Mo and V films are preferentially grown in the (110) direction (Fig. 8(a)), the difference in the surface morphologies is not very obvious, as shown in Figs. 8(b) and 8(c). Both surfaces are covered with dense worm-like grains, but the grain size of the film covered with V is more uniform than that of Mo surface and the number of pores between grains is reduced. From the cross-sectional view in Fig. 8(d), we can see that the bond between V film and Mo substrate is very good, and no holes and gaps are formed at the Mo/V interface.

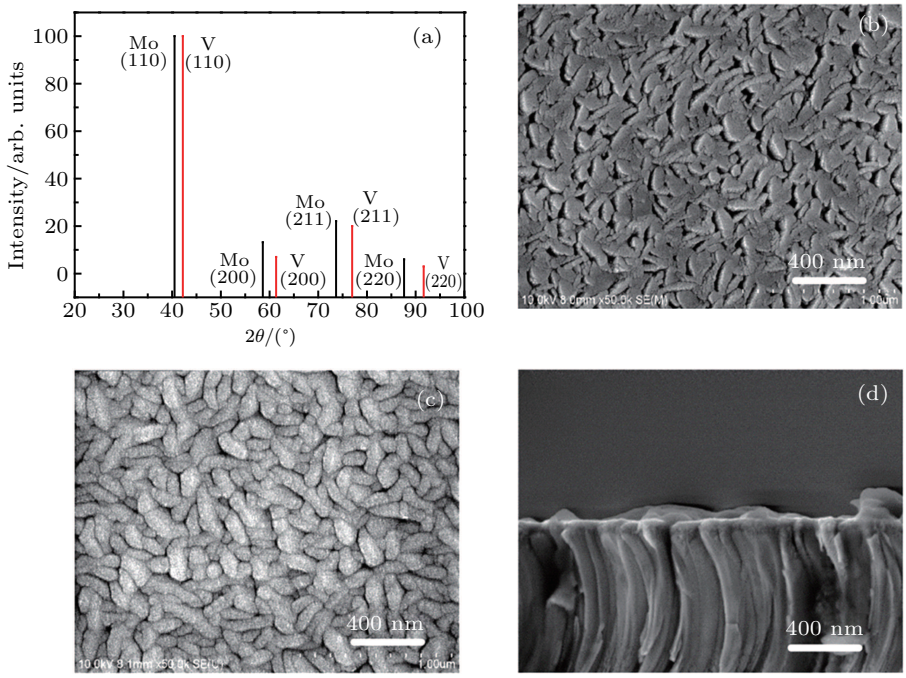


Fig. 8. (a) XRD patterns of Mo and V standard diffraction peaks, (b) SEM image of the Mo film, (c) vanadium film prepared on Mo substrate, (d) cross-sectional view of the vanadium film prepared on Mo substrate.

The V film prepared on Mo substrate was then selenized at the temperature of 400 °C. Figure 9(a) shows the XRD pattern of the sample. Due to the strong Mo diffraction peak, the diffraction peaks of others are too weak. In order to analyze the other phase, we cut off the Mo diffraction peak positioned at about $2\theta = 39°$–$42°$. It is obvious that the (001) and (002) crystal phases of VSe_2 can also be obtained on the Mo substrate. At the same time, it also generates $MoSe_2$. This happens because Se diffuses so fast that the VSe_2 layer does not block the Se contacting with Mo to form $MoSe_2$. The de-

tailed morphologies and microstructures of the as-synthesized VSe_2 nanosheets were investigated using SEM, as shown in Fig. 9(b). The surface of the sample is covered with a number of hexagonal nanosheets. It is also consistent with the morphology of the VSe_2 prepared on the glass substrate. It shows that the stability of our two-step preparation of VSe_2 process is very good.

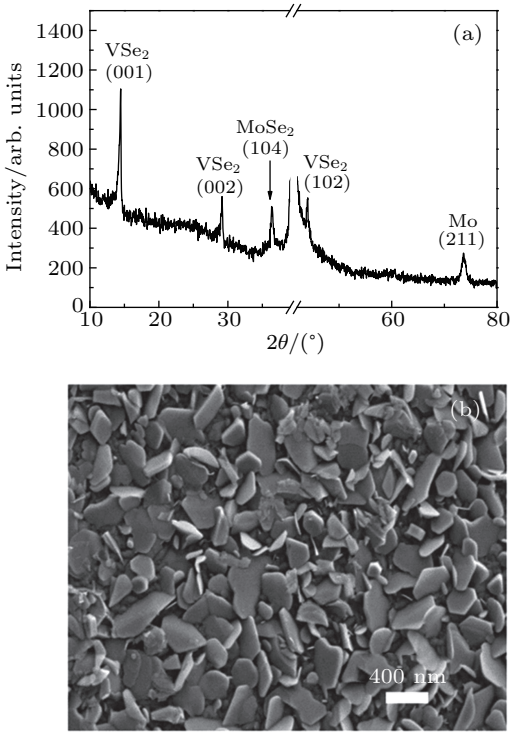


Fig. 9. (a) XRD pattern and (b) SEM image of the VSe_2 prepared on Mo substrate.

To understand the contact properties between Mo (metal) substrate and VSe_2 (semiconductor material), we prepared a certain thickness of Al electrode on the Mo surface and VSe_2 surface, and then performed the dark state *I*–*V* test. In Fig. 10, the black curve represents the contact between Al/Mo, and the red represents the contact between Al/VSe_2/Mo. It can be seen that the *I*–*V* curve of the Al/Mo substrate is linear, which is a typical *I*–*V* characteristic curve of ohmic contact. That is to say, the contact characteristic between Al and Mo is ohmic. The *I*–*V* curve of the sample with the VSe_2 film is also a linear straight line, so it can be concluded that there is ohmic contact between Al and VSe_2 and Mo. This result shows that VSe_2 can be well applied to semiconductor devices because of its good ohmic contact.

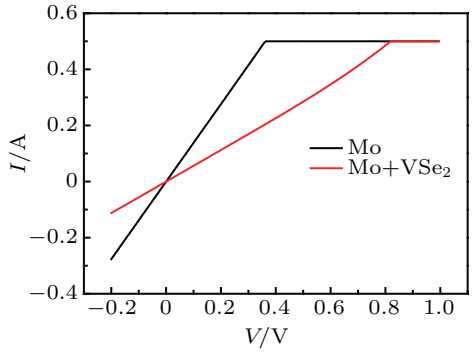


Fig. 10. Metal–semiconductor contact *I*–*V* curve between Mo/Al and Al/VSe_2/Mo.

In addition, we also performed a Hall test on the above samples. The test results are summarized in Table 1. The sample with VSe_2 (0.2102 Ω/sq) has a lower square resistance than the molybdenum substrate without VSe_2 (0.2135 Ω/sq). However, compared to the Mo substrate, the mobility of electrons is reduced. Because the carrier concentration of the VSe_2 sample can reach the order of 10^{18}. VSe_2 can be well applied in semiconductor devices.

Table 1. The Hall measurements of Mo substrate and VSe_2 films prepared on Mo substrate.

Sample	Sheet resistance/(Ω/sq)	Coefficient/$m^2 \cdot C^{-1}$	Mobility/$cm^2 \cdot V^{-1} \cdot s^{-1}$	Carrier concentration/cm^{-2}
Mo	0.2135	0.000699	32.8	8.93×10^{17}
Mo+VSe_2	0.2102	0.000269	12.8	2.32×10^{18}

4. Conclusion and perspectives

In summary, we demonstrate a new two-step route to synthesize the VSe_2 film. By comparing the different selenization temperatures, we find that the VSe_2 film has the best crystal quality when the selenization temperature is 400 °C. At 400 °C selenization temperature, we can stably prepare VSe_2 film on both glass and Mo substrates. The XRD patterns of the VSe_2 film indicate the VSe_2 preferential growth along the *c*-axis. A number of hexagonal nanosheets can be clearly seen from the SEM image. Moreover, the sample of V thin film selenized at 400 °C has the highest reflectivity and the lowest transmittance. This indicates that VSe_2 is well suited for application in optoelectronic devices. In addition, the contact between Al/VSe_2/Mo belongs to ohmic contact, and the lower square resistance of VSe_2/Mo sample can be observed. VSe_2 is a potential material for solar cells. Moreover, this work opens up the opportunity for extensive research on the application of VSe_2 in photovoltaic device or other semiconductor material devices.

References

[1] Manzeli S, Ovchinnikov D, Pasquier D, Yazyev O and Kis A 2017 *Nat. Rev. Mater.* **2** 17033

[2] Tan C, Lai Z and Zhang H 2017 *Adv. Mater.* **29** 1701392

[3] Lin X and Wang J 2017 *Acta Chim. Sin.* **75** 979

[4] Novoselov K S, Mishchenko A, Carvalho A and Castro Neto A H 2016 *Science* **353** 9439
[5] Zhao W, Dong B, Guo Z L, Su G, Gao R J, Wang W and Cao L X 2016 *Chem. Commun. (Camb)* **52** 9228
[6] Xu K, Chen P Z, Li X L, Wu C Z, Guo Y Q, Zhao J Y, Wu X J and Xie Y 2013 *Angew Chem. Int. Ed Eng.* **52** 10477
[7] Marri S R, Ratha S, Rout C S and Beheraet J N 2017 *Chem. Commun. (Camb)* **53** 228
[8] Vatansever E, Sarikurt S and Evans R F L 2018 *Mater. Res. Express* **5** 046108
[9] Bonilla M, Kolekar S, Ma Y, Diaz H C, Kalappattil V, Das R, Eggers T, Gutierrez H R, Phan M H and Batzillet Ma 2018 *Nat. Nanotechnol* **13** 289
[10] Zhang Z P, Niu J J, Yang P F, Gong Y, Ji Q Q, Shi J P, Fang Q Y, Jiang S L, Li H, Zhou X B, Gu L, Wu X S and Zhang Y F 2017 *Adv. Mater.* **29** 1702359
[11] Hayashi K and Nakahira M 1978 *J. Soild State Chem.* **24** 153
Hayashi K and Nakahira M 1978 J.Solid State Chem. 24 153
[12] Whittingham M S 1978 *Mat. Res. Bull.* **13** 959
[13] Nikonov K S, Brekhovskikh M N, Egorysheva A V, Menshchikova T K and Fedorovet V A 2017 *Inorg. Mater.* **53** 1126
[14] Yang J Y, Wang W K, Liu Y, Du H F, Ning W, Zheng G L, Jin C, Han Y Y, Wang N, Yang Z R, Tian M L and Zhang Y H 2014 *Appl. Phys. Lett.* **105** 063109
[15] Claessen R, Schafert I and Skibowski M 1990 *J. Phys.: Condens. Matter* **2** 10045
[16] Hossain M, Wu J X, Wen W, Liu H N, Wang X S and Xie L M 2018 *Adv. Mater. Interfaces* **5** 1800528
[17] Wang C L, Wu X, Ma Y H, Mu G, Li Y Y, Luo C, Xu H J, Zhang Y Y, Yang J, Tang X D, Zhang J, Bao W Z and Duan C G 2018 *J. Mater. Chem. A* **6** 8299
[18] Hector A L, Jura K, Levason W, Reid S D and Reidet G 2009 *New J. Chem.* **33** 641
[19] Zhang Z P, Gong Y, Zou X L, Liu P, Yang P F, Shi J P, Zhao L Y, Zhang Q, Gu L and Zhang Y F 2018 *ACS Nano*
[20] Lee S, Kim J, Park Y C and Chun S H 2019 *Nanoscale* **11** 431
[21] Ming F W, Liang H F, Lei Y J, Zhang W L and Alshareef H N 2018 *Nano Energy* **53** 11
[22] Lin H, He S J, Mao Z, Miao J, Xu M and Li Q 2017 *Nanotechnology* **28** 445603
[23] Wang Y P, Qian B B, Li H H, Liu L, Chen L and Jiang H B 2015 *Mater. Lett.* **141** 35
[24] Wang D L, Bai Z Z, Yang R L and Hou Z R 2013 *Physics* **42** 346
[25] Gao S S, Jiang Z W, Wu L, Ao J P, Zeng Y, Sun Y and Zhang Y 2018 *Chin. Phys. B* **27** 018803
[26] Liu Z L, Wu X, Shao Y, Qi J, Cao Y, Huang L, Liu C, Wang J O, Zheng Q, Zhu Z L, Ibrahim K, Wang Y L and Gao H J 2018 *Sci. Bull.* **63** 419
[27] Ulusoy Ghobadi T, Patil B, Karadas F, Okyay A K and Yilmaz E 2017 *ACS Omega.* **2** 8319
[28] Cao Q, Frank F Y, Lina S, Xiang F X, Liu G L and Wang X L 2017 *Nanotechnology* **28** 475703